Three-Photon Absorption Cross-Section Enhancement in Two Symmetrical Fluorene-Based Molecules

Junhui Liu,* Yanli Mao, Mingju Huang, Yuzong Gu, and Weifeng Zhang

Institute of Microsystem of Physics, Department of Physics and Electronics, Henan University, Kaifeng, Henan 475001, P. R. China

Received: May 15, 2007; In Final Form: July 13, 2007

In this article, we report the pure three-photon absorption effects of two novel symmetrical fluorene-based molecules with 2D−π−2D [9,9-diethylhexyl-2,7-bis-(*N*,*N*-diphenylamine)fluorene] and 2D−D−π−D−2D [5,5′-(9,9-bis-(2-ethylhexyl)-9H-fluorene-2-yl)bis(*N*,*N*-diphenylthiophen-2-amine)] structural motifs. The obtained three-photon absorption cross sections, $(4.74 \pm 0.01) \times 10^{-76}$ and $(6.77 \pm 0.02) \times 10^{-76}$ cm^6 s^2 for the 2D−π−2D and 2D−D−π−D−2D archetypes, respectively, are rather high. The geometries and electronic excitations of the two molecules were systematically studied by the PM3 and ZINDO/S methods. The influence of the different molecular structures on the three-photon absorption cross section is discussed micromechanically. The experimental and theoretical results demonstrate that the transition dipole moment between the ground and final states is the most definitive factor. A new fitting method that is more accurate than those reported previously was used to obtain the 3PA coefficient.

1. Introduction

In the early 1930s, multiphoton absorption of an atom was introduced into the literature as a new concept by Göppert-Mayer.[1] The two-photon absorption (TPA) process could produce a spatially confined excitation useful for numerous technological applications.[2,3] The success of the two-photon technology created much interest in exploring applications based on three-photon absorption (3PA). 3PA is becoming an intriguing possibility because of its potential applications in the photonics, biomedical, and light-activated therapy fields.[4−6] 3PA refers to the simultaneous absorption of three photons in a single event through virtual states.[7] In organic molecules, 3PA typically occurs at longer wavelengths in the near-infrared (NIR) region. This introduces some advantages, including minimization of the scattered light losses and reduction of undesirable linear absorption,[8] so that a greater penetration depth and less damage in some materials can be obtained. Consequently, molecules with large 3PA cross sections can be easily applied in the fields of multiphoton fluorescence imaging,[9−11] upconverted stimulated emission,[12] optical limiting,[13−15] and so on. The cubic dependence of 3PA processes on the incident light intensity provides stronger spatial confinement, so that a higher contrast in imaging can be obtained than with the TPA process.[16−18]

However, the relatively small 3PA cross section, σ_3', values of current nonlinear organic molecules have deferred their practical applications. Only a few systematic experimental and theoretical studies have been reported. There is still a lack of fundamental information on the molecular structure/property relations, and therefore, the foundations to provide the basis for molecular engineering remain in great need. Much effort toward studies on 3PA in organic molecules has been undertaken in recent years. Using a donor with stronger withdrawing character and increasing the conjugation length can enhance the 3PA cross sections.[19]

In this article, we investigate the 3PA-induced upconversion fluorescence emission and the 3PA cross section of two novel fluorene-based molecules with the symmetric 2D−π−2D and 2D−D−π−D−2D conjugated structures, which are identified as 9,9-diethylhexyl-2,7-bis-(*N*,*N*-diphenylamine)fluorene and 5,5′-(9,9-bis-(2-ethylhexyl)-9H- fluorene-2-yl)bis(*N*,*N*-diphenylthiophen-2-amine), respectively. These two molecules were both synthesized in our laboratory by the method of Cu-mediated Ullmann condensation reactions.[20] D and π represent the electron donor and the conjugated π-electron bridge, respectively. The 2D−π−2D molecule has two electron donors on each side and was transformed into the 2D−D−π−D−2D structure by inserting two thiophen rings, one on each side of the fluorene core, and their molecular structures are shown in Figure 1. It was observed that the two molecular structures had a large influence on the 3PA effect. To provide useful information for the design of large 3PA materials, we focused on gaining insight into the effect of donor groups on the 3PA properties of these fluorene-based molecules. At the same time, we also made great efforts to study the fitting method of 3PA coefficient.

2. Results and Discussion

2.1. Linear Absorption and Steady-State Fluorescence Emission. Figure 2 shows the linear absorption and steady-state fluorescence spectra of 2D−π−2D and 2D−D−π−D−2D in DMF at a concentration of 1.4×10^{-5} mol/L, measured using a UV−vis−NIR Cary5000 spectrophotometer and a Spex fluorescence spectrometer, respectively. The influences from the quartz liquid cell and the solvent have been subtracted. The two molecules show strong UV absorption in the spectral ranges of 260−400 nm for 2D−π−2D and 260−480 nm for 2D−D−π−D−2D, but no linear absorption in longer-wavelength ranges. This indicates that excitation in longer-wavelength ranges can occur only through multiphoton absorption processes. On the other hand, by comparing the maximum absorption wavelength and the spectral position of the maximum absorption peak, one

* To whom correspondence should be addressed. Tel.: 0086-378-3881602. Fax: 0086-378-3881602. E-mail: junhuiliu@henu.edu.cn.

10.1021/jp073711t CCC: $37.00
Published on Web 08/28/2007

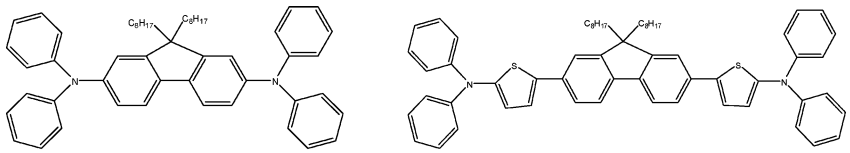

(a) (b)

Figure 1. Molecular structures of (a) 9,9-diethylhexyl-2,7-bis-(*N*,*N*-diphenylamine)fluorene(2D−π−2D) and (b) 5,5′-(9,9-bis-(2-ethylhexyl)-9H-fluorene-2-yl)bis(*N*,*N*-diphenylthiophen-2-amine) (2D−D−π−D−2D).

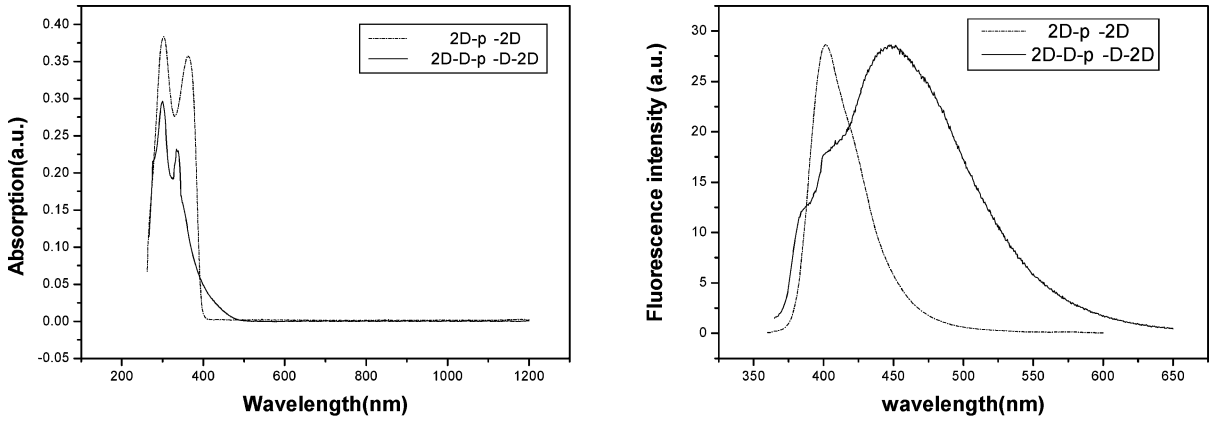

(a) (b)

Figure 2. Linear absorption and steady-state fluorescence spectra of 2D−D−π−D−2D (solid line) and 2D−π−2D (dash-dotted line) in DMF at 1.4×10^{-5} mol/L.

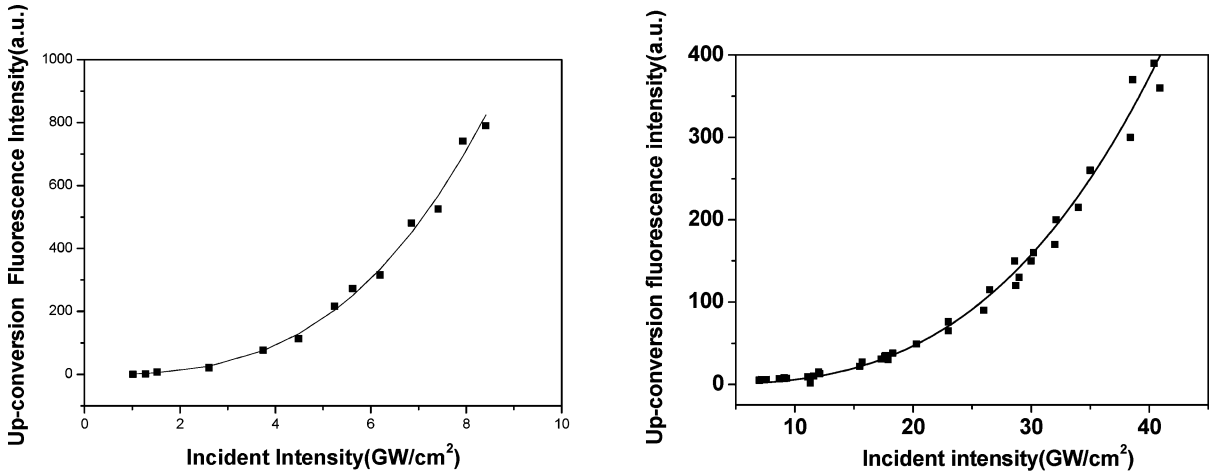

(a) (b)

Figure 3. Cubic dependence of the 3PA-induced fluorescence intensity vs incident intensity at 1064 nm for (a) 2D−π−2D and (b) 2D−D−π−D−2D in DMF. The solid lines are the best-fit curves based on the function $y = ax^n$.

can predict that the two molecules should have similar transitions from ground state to excited state but that a lower excitation energy is needed for 2D−D−π−D−2D than for 2D−π−2D.

2.2. Three-Photon-Induced Fluorescence. In the measurement of the upconversion fluorescence of the two compounds, the incident 1064-nm laser excitation was provided by a Q-switched Nd:YAG pulsed laser (Continuum, PY61-10) with a pulse width of 38 ps and a repetition rate of 10 Hz. A blue fluorescence emission could be readily observed by human eyes when the incident intensity reached several hundred megawatts per square centimeter. The shapes of the steady-state and upconversion fluorescence are virtually identical for each compound (data not included). These results reveal that the radiative relaxation processes take place from the same excited state for each molecule regardless of the excitation process. A characteristic feature of the 3PA-induced fluorescence is the cubic dependence of the fluorescence intensity on the incident laser intensity. To corroborate the order of the excitation process, we measured the emission intensity vs incident intensity (as shown in Figure 3). The upconversion fluorescence intensity, measured at the maximum emission wavelengths of 400 nm for 2D−π−2D and 440 nm for 2D−D−π−D−2D, exhibits a cubic dependence on incident intensity through the relation $y = ax^n$. The best-fit exponents were found to be 2.96 and 2.98 (within admissible error), respectively, as is characteristic of three-photon processes. The possibility of excited-state absorp-

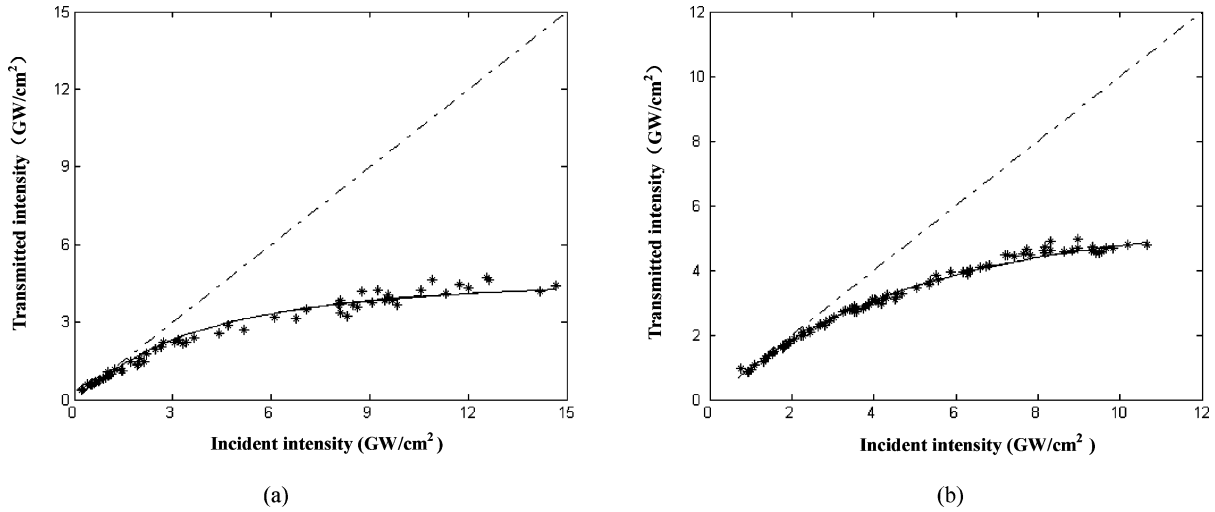

Figure 4. Transmitted intensity vs incident intensity of (a) 2D−π−2D and (b) 2D−D−π−D−2D with fittings using method 1. The dash-doted lines are the fitted curves with $\gamma = 0$. The solid lines represent the theoretical fittings. The best-fit parameters were (a) $\gamma = 10.7 \times 10^{-20}$ cm^3/W^2 and (b) $\gamma = 8.19 \times 10^{-20}$ cm^3/W^2.

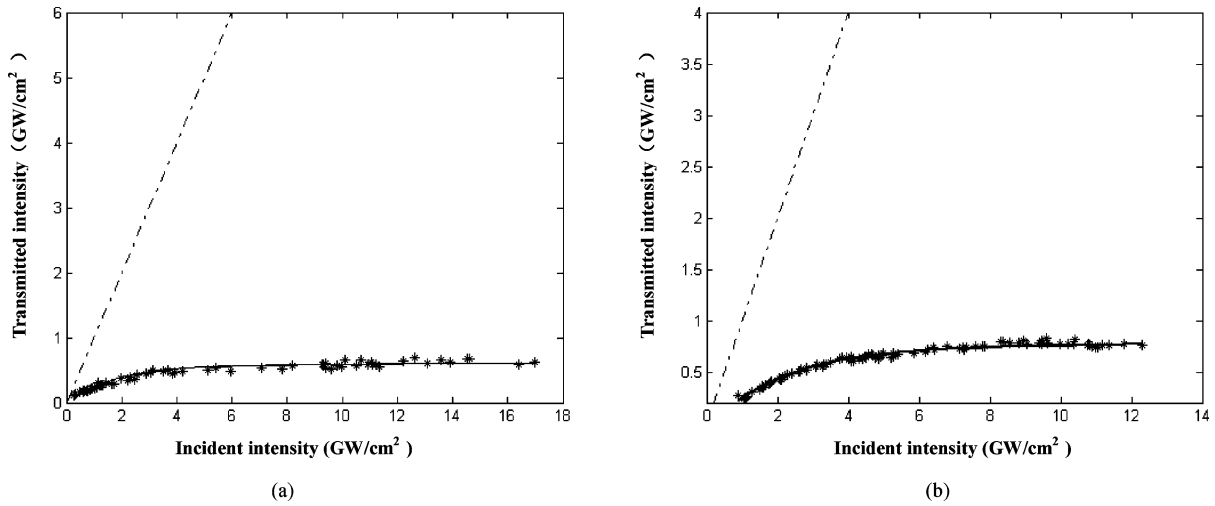

Figure 5. Transmitted on-axis intensity vs incident on-axis intensity of (a) 2D−π−2D and (b) 2D−D−π−D−2D, with fittings using method 2. The dash-dotted lines are the best-fit curves with $\gamma = 0$. The solid lines represent the theoretical fittings. The best-fit parameters were (a) $\gamma = 22.9 \times 10^{-20}$ cm^3/W^2 and (b) $\gamma = 17.5 \times 10^{-20}$ cm^3/W^2.

tion can be discarded, on one hand, because the lifetime of the excited state on the two molecules is in the nanosecond range, so that there is no time for excited-state absorption during the pulse.[21] On the other hand, because of the absence of absorption of 1PA (1064 nm) and 2PA (532 nm) at the working wavelength of 1064 nm (as shown in Figure 2a), there is no intermediate state between the ground state and the excited state even though picosecond pulses are employed.[8] One can be confident that the excitation processes are induced by the simultaneous absorption of three photons.

2.3. Three-Photon Absorption Cross Section. The measurements of the 3PA coefficient of 2D−π−2D and 2D−D−π−D−2D in DMF solution at 2.8×10^{-2} mol/L and 1.5×10^{-2} mol/L, respectively, were done in a 10-mm-long quartz cell, pumping with the same laser described above. The pump energy was controlled by a continuous attenuator. The IR laser beam was separated into two beams by a beam splitter. One beam was detected directly by a J3-05 probe (made by Molectron Co.) to monitor the incident laser pulse energy, and the other was focused into the quartz cell by a 25.6-cm-long-focus convex lens (the quartz cell was 10 mm behind the focusing plane). The beam waist at the focal plane was 26 μm. The entire transmitted energies through the sample were totally collected into another J3-05 probe by a lens. The high σ_3' values of the two compounds were obtained with intensity-dependent transmittance measurements (Figures 4 and 5), fit according to the following methods.

2.3.1. Method 1. According to the definition of the absorption coefficient, the intensity change of an excitation beam along optical propagation path z is given by

$$dI(z)/dz = -\gamma I^3(z) - \beta I^2(z) - \alpha I(z) \quad (1)$$

where γ, β, and α are, respectively, the 3PA, TPA, and 1PA coefficients of the given sample in the medium and $I(z)$ is the irradiance, which depends on the propagation distance z. If the linear absorption and 2PA are negligible and 3PA is the only process involved, the above equation can be rewritten simply as

$$dI(z)/dz = -\gamma I^3(z) \quad (2)$$

The solution of eq 2 is

$$I(z) = I_0/(1 + 2\gamma z I_0^2)^{1/2} \quad (3)$$

TABLE 1: 3PA Coefficients, 3PA Cross Sections, and Minimum Transmittances (T_m) of the Two Compounds Estimated Using Methods 1 and 2

	$\gamma \times 10^{-20}$ (cm^3/W^2)		$\sigma_3' \times 10^{-76}$ (cm^6 s^2)		T_m (%)	
molecules	method 1	method 2	method 1	method 2	method 1	method 2
2D−π−2D	10.7	22.9	2.22	4.74	29	3.5
2D−D−π−D−2 D	8.19	17.5	3.17	6.77	45	6.3

where I_0 is the incident irradiance of the excitation beam and z is the propagation distance within the sample medium. We assume an equivalent rectangular pulse shape to give a rough estimate of intensity I_0 or $I(z)$.[13] Equation 3 can be solved numerically for the 3PA coefficient γ with a given z value. Figure 4 shows the curves of the transmitted intensity vs incident intensity for the two fluorene derivatives. Each data point represents an average over 30 laser pulses. The solid lines represent the theoretical fittings with the best-fit parameter γ for each molecule. The corresponding values are reported in Table 1.

2.3.2. Method 2. Assuming a Gaussian beam traveling along the $+z$ direction (the origin of the z coordinate is located at the focusing plane), the irradiance can be written as

$$I(z,r) = \frac{{A_0}^2}{\omega^2(z)} \exp\left[-\frac{2r^2}{\omega^2(z)}\right] \tag{4}$$

where $\omega^2(x) = \omega_0^2[(1 + (\lambda z/\pi\omega_0^2 n)^2]$, ω_0 is the waist radius of the Gaussian beam, λ is the laser wavelength, and A_0^2/ω_0^2 is the on-axis irradiance of the Gaussian beam at the focus. $I(z,r)$ is the irradiance, which depends on the propagation distance z and the beam intensity radial r.

Now, we consider a rectangular light beam (not a Gaussian beam) traveling in the $+z$ direction within a nonlinear sample exhibiting 3PA. The light beam propagating through the sample is governed by the equation

$$\mathrm{d}I(z',r,t)/\mathrm{d}z' = -\gamma I(z',r,t)^3 \tag{5}$$

where z' is the propagation length inside the sample. The solution for eq 5 is

$$I(L,r,t) = \frac{I(z=0,r,t)}{\sqrt{1 + 2\gamma L I^2(z=0,r,t)}} \tag{6}$$

It is well-known that a Gaussian beam propagates in the collective or dispersing direction, i.e., r in eq 4 is not a constant. Therefore, if the data are simply fitted with eq 6, a considerable error cannot be avoided, particularly in a thick sample.

However, if the sample length is small enough that the changes of the beam diameter within the sample can be neglected, the medium can be regarded as "thin", in which case one can use eq 6 to fit the experimental curves. However, the questions remain: How does the thickness influence 3PA? How can one fit the data from a thick sample, such as in our experiments?

We divide the sample passed by the laser into m cylinders along the z direction and divide each cylinder into n annuluses along the r direction; hence, there are $m \times n$ annuluses in the sample. The light intensity in a given annulus is assumed to be homogeneous along the r direction and parallel along the z direction, so that eq 6 can be used for all of the annuluses.

$$I''(i,j,t) = \frac{I'(i,j,t)}{\sqrt{1 + 2\gamma L' I'^2(i,j,t)}}$$

$$I'(i,j+1,t) = \frac{S''(i,j)}{S'(i,j+1)} I''(i,j,t)$$

$$T = \frac{\sum_{i=1}^{i=n} I''(i,m,t) S''(i,m) t_p}{\sum_{i=1}^{i=n} I'(i,1,t) S'(i,1) t_p} \tag{7}$$

Here $L' = L/m$ is the thickness of each annulus, L is the distance traveled by the beam through the sample, and t_p is the pulse width. $I'(i,j,t)$ is the incident irradiance at the front side of the (i,j) annulus; $I''(i,j,t)$ is the transmitted irradiance of the same annulus; and $S''(i,j)$ and $S'(i,j+1)$ are the area of the exit plane of the annulus and the area of the incident plane of the next annulus, respectively. After the experimental curves for a given i and j value are fit, the 3PA coefficients γ can be obtain. When larger values for i and j are used, the γ value obtained is more accurate. By comparing the computational data, the results indicate that the error is ca. 1‰ at $i = j = 10^3$, and ca. 0.05‰ at $i = j = 10^4$. Interestingly, one can obtain the light intensity I at any position in the samples with this method. Figure 5 shows the transmitted on-axis intensity vs the incident on-axis intensity for the two compounds. The solid lines represent the theoretical fittings with the best-fit parameters γ listed in Table 1.

By comparing the two fitting results obtained with the above two methods, one can find many differences between them. For instance, the transmitted maximum light intensities from method 2 are less than 0.7 GW/cm^2 for 2D−π−2D and 2D−D−π−D−2D, but the values from method 1 are both more than 5 GW/cm^2 for the two compounds. Second, as for 2D−D−π−D−2D, the transmittance from method 2, which is 24.7% with an incident intensity of 0.89 GW/cm^2 and 6.3% with an incident intensity of 12.3 GW/cm^2, is considerably lower than that from method 1, namely 45% with an incident intensity of 10.6 GW/cm^2. Simultaneously, it also means the two dyes are a promising type of optical limiting material induced by 3PA in the near-infrared spectra regions. Third, the γ values from method 2 are almost 2 times greater than those from method 1. The discrepancy between the two methods is given by the fact that the theoretical fitting for method 1 assumes an equivalent rectangular pulse shape to give a rough estimate of intensity I_0 or I_z instead of a Gaussian distribution.

The molecular 3PA absorption cross section σ_3' for a given sample in solution is obtained with the units of cm^6 s^2, after relating γ to the solute concentration d_0 (mol/L) and the photon energy hc/λ by

$$\sigma_3' = \frac{\gamma}{N_A d_0 \times 10^{-3}} \left(\frac{hc}{\lambda}\right)^2 \tag{8}$$

where N_A is Avogadro's constant. The intrinsic sample molecular 3PA cross sections can be estimated as (4.74 ± 0.01) ×

TABLE 2: Electronic Transition Data Obtained by the ZINOD/S Semiempirical Method for the Two Molecules at the AM1-Optimized Geometry

electronic transition	excitation energy (eV)	λ^a (nm)	transition electric dipole moments (au)			f^c
			X^b	Y	Z	
			2D−π−2D			
$S_0 \rightarrow S_1$	3.7471	330.88	−2.9800	0.0176	0.1088	0.8164
$S_0 \rightarrow S_2$	3.9873	310.95	0.3317	−0.5105	−0.1103	0.0374
$S_0 \rightarrow S_3$	4.0841	303.58	0.3644	0.2598	−0.0875	0.0208
$S_0 \rightarrow S_4$	4.3297	286.36	−0.1877	−0.2342	−0.3756	0.0245
$S_0 \rightarrow S_5$	4.3902	282.41	−0.4524	−0.4379	0.3176	0.0535
$S_0 \rightarrow S_6$	4.4122	281.00	−0.2512	−0.3931	0.4696	0.0474
			2D−D−π−D−2D			
$S_0 \rightarrow S_1$	3.1021	399.68	−4.6639	0.0084	−0.1031	1.6539
$S_0 \rightarrow S_2$	3.5004	354.20	−0.4329	0.4088	0.3657	0.0419
$S_0 \rightarrow S_3$	3.9145	316.73	0.1556	0.1775	0.0125	0.0054
$S_0 \rightarrow S_4$	3.9898	310.76	0.1823	−0.1521	−0.0745	0.0061
$S_0 \rightarrow S_5$	4.1472	298.96	−0.4555	−0.0886	0.1103	0.0231
$S_0 \rightarrow S_6$	4.3413	285.59	0.2888	−0.0882	0.4447	0.0307

[a] λ values are from ZINDO computations. [b] X is the long molecular axis. [c] Oscillator strength.

10^{-76} cm^6 s^2 and (6.77 ± 0.02) × 10^{-76} cm^6 s^2 for the 2D−π−2D and 2D−D−π−D−2D archetypes, respectively (as reported in Table 1).

The obtained three-photon absorption cross sections for the two symmetrical fluorene-based molecules are quite high, especially for 2D−D−π−D−2D. The measured σ_3' value is larger than that of the symmetrical A−π−A compound,[21] larger than that of stilbazolium-like derivatives under similar experimental conditions,[14] and comparable to that of BBTDOT excited by nanosecond pulses.[13] The large values of σ_3' are the result of the electron delocalization along the molecular system, large π-electron conjugation, and strong electron donors.

It can easily be found that the σ_3' values are strongly related to the chemical structures of the two compounds by comparison. The difference between the two molecules is the form of the electron donors, because of which the σ_3' values are much enhanced by a factor of 1.4. It is significant to clarify the influence of electron donors on the 3PA cross section, so as to offer more useful information to further synthesis of new materials with larger σ_3' values.

2.4. Ground-to-Excited-State Transition Processes. Quantum chemistry calculations were performed on an Intel (2.8 Hz) personal computer with 512 MB of RAM using the Gaussian 03W program. Optimized ground-state geometries of the two fluorene-based molecules were obtained by the AM1 method. The ZINDO/S semiempirical method was employed to obtain their energy and the transition dipole moments of the first six singlet−singlet electronic transitions. The electronic transition data are reported in Table 2. It can be seen that the oscillator strength (f) and the transition dipole moment along the long axis of the molecule (X) of the $S_0 \rightarrow S_1$ electronic transition are the largest for the two molecules, which indicates that the first excited state, S_1, is the strongest one-photon absorption state. A strong one-photon absorption state can be a strong 3PA state as well.[22] From Table 2, one can see that the transition dipole moment, μ^{0f}, between the ground state and the first excited state along the X axis were determined for both symmetric molecules, yielding μ^{0f}(2D−π−2D) = 2.98 (au) and μ^{0f}(2D−D−π−D−2D) = 4.6639 (au), which are in proportion to the 3PA cross sections. These results reveal that the transition dipole moment between the ground state and the final state, μ^{0f}, is the most definitive factor.

We can easily find that the inclusion of the two thiophen rings in 2D−D−π−D−2D increased the transition dipole moment between the ground state and the final state, μ^{0f}, and therefore, enhanced the 3PA cross section by comparing the two molecular structures.

3. Conclusions

In summary, the 3PA of two novel symmetrical charge-transfer fluorene-based molecular structures, 2D−π−2D and 2D−D−π−D−2D, was demonstrated. A new and precise fitting method was employed to obtain the 3PA cross sections of the two molecules, which are 4.74 × 10^{-76} and 6.77 × 10^{-76} cm^6 s^2, respectively. Semiempirical calculations of the transition dipole moment between the ground state and the excited state were performed using the ZINDO/S method. The experimental and theoretical results of this study demonstrate that the first excited state, S_1, is the strongest 3PA state for the two molecules and that the transition dipole moment between the ground state and final state (S_1), μ^{0f}, is the most definitive factor for 3PA, by which the 3PA cross section can be increased.

Acknowledgment. This work was supported by the Project of Cultivating Innovative Talents for Colleges and Universities of Henan Province, China, and the Foundation for University Key Teachers of Henan Province, China. The authors acknowledge Dr. Wenbo Ma for his assistance.

Supporting Information Available: Experimental setup used to measure the three-photon-induced frequency-upconversion fluorescence. This material is available free of charge via the Internet at http://pubs.acs.org.

References and Notes

(1) Göppert-Mayer, M. Über Elementarakte mit zwei Quantensprüngen. *Ann. Phys.* **1931**, *9*, 273−294.

(2) Perry, J. W.; Mansour, K.; Marder, S. R.; Perry, K. J.; Alvarez, D., Jr.; Choong, I. Enhanced reverse saturable absorption and optical limiting in heavy-atom-substituted phthalocyanines. *Opt. Lett.* **1994**, *19*, 625−627.

(3) Cumpston, B. H.; Ananthavel, S. P.; Barlow, S.; Dyer, D. L.; Ehrlich, J. E.; Erskine, L. L.; Heikal, A. A.; Kuebler, S. M.; Lee, I.-Y. S.; McCord-Maughon, D.; Qin, J.; Röckel, H.; Rumi, M.; Wu, X.-L.; Marder, S. R.; Perry, J. W. Two-photon polymerization initiators for three-dimensional optical data storage and microfabrication. *Nature* **1999**, *51*, 378.

(4) Cable, J. R.; Albrecht, A. C. A condensed phase study of the benzene $B_{2u} \leftarrow A_{1g}$ three-photon transition. *J. Chem. Phys.* **1986**, *8*, 3155−3164.

(5) Meyer, H. Determination of ground state populations and alignment parameters using nonresonant three-photon absorption. *J. Chem. Phys.* **1995**, *102*, 3110−2112.

(6) Davey, A. P.; Bourdin, E.; Henari, F.; Blau, W. Three photon induced fluorescence from a conjugated organic polymer for infrared frequency upconversion. *Appl. Phys. Lett.* **1995**, *67*, 884−885.

(7) Singh, S.; Bradley, L. T. Three-Photon Absorption in Napthalene Crystals by Laser Excitation. *Phys. Rev. Lett.* **1964**, *12*, 612−614.

(8) Hernández, F. E.; Belfield, K. D.; Cohanoschi, I. Three-photon absorption enhancement in a symmetrical charge transfer fluorene derivative. *Chem. Phys. Lett*. **2004**, *391*, 22−26.

(9) Maiti, S.; Shear, J. B.; Williams, R. M.; Zipfel, W. R.; Webb, W. W. Measuring Serotonin Distribution in Live Cells with Three-Photon Excitation. *Science* **1997**, *275*, 530−532.

(10) Szmacinski, H.; Gryczynski, I.; Lakowicz, J. R. Three-photon induced fluorescence of the calcium probe Indo-1. *Biophys. J.* **1996**, *70*, 547−555.

(11) Gu, M. Resolution in three-photon fluorescence scanning microscopy. *Opt. Lett.* **1996**, *21*, 988−910.

(12) He, G. S.; Markowicz, P. P.; Lin, T.-C.; Prasad, P. N. Observation of stimulated emission by direct three-photon excitation. *Nature* **2002**, *415*, 767−770.

(13) He, G. S.; Bhawalkar, J. D.; Prasad, P. N. Three-photon-absorption-induced fluorescence and optical limiting effects in an organic compound. *Opt. Lett.* **1995**, *20*, 1524−1526.

(14) Wang, D.-Y.; Zhan, C.-L.; Chen, Y.; Li, Y.-J.; Lu, Z.-Z.; Nie, Y.-Z. Large optical power limiting induced by three-photon absorption of two stilbazolium-like dyes. *Chem. Phys. Lett.* **2003**, *369*, 621−626.

(15) Mao, Y.; Liu, J.; Ma, W.; Wu, Y.; Cheng, Y. Three-photon absorption-induced fluorescence and optical limiting effects in a fluorene derivative. *J. Mod. Opt.* **2007**, *54*, 77−84.

(16) Albota, M.; Beljonne, D.; Brédas, J.-L.; Ehrlich, J. E.; Fu, J.-Y.; Heikal, A. A.; Hess, S. E.; Kogej, T.; Levin, M. D.; Marder, S. R.; McCord-Maughon, D.; Perry, J. W.; Röckel, H.; Rumi, M.; Subramaniam, G.; Webb, W. W.; Wu, X.-L.; Xu, C. Design of Organic Molecules with Large Two-Photon Absorption Cross Sections. *Science* **1998**, *281*, 1653−1656.

(17) Cumpston, B. H.; Ananthavel, S. P.; Barlow, S.; Dyer, D. L.; Ehrlich, J. E.; Erskine, L. L.; Heikal, A. A.; Kuebler, S. M.; Lee, I.-Y. S.; McCord-Maughon, D.; Qin, J.; Röckel, H.; Rumi, M.; Wu, X. L.; Marder, S. R.; Perry, J. W. Two-photon polymerization initiators for three-dimensional optical data storage and microfabrication. *Nature* **1999**, *398*, 51−54.

(18) Zhou, W.; Kuebler, S. M.; Braun, K.; Yu, T.; Cammack, J. K.; Ober, C.; Perry, J. W.; Marder, S. R. An Efficient Two-Photon-Generated Photoacid Applied to Positive-Tone 3D Microfabrication. *Science* **2002**, *296*, 1106−1109.

(19) Ma, W.; Wu, Y.; Han, J.; Gu, D.; Gan, F. Large three-photon absorption cross section in a novel class of bis-(N-carbazolyl) fluorene derivatives. *Chem. Phys. Lett.* **2005**, *403*, 405−409.

(20) Belfield, K. D.; Schafer, K.J.; Mourad, W.; Reinhardt, B. A. Synthesis of New Two-Photon Absorbing Fluorene Derivatives via Cu-Mediated Ullmann Condensations. *J. Org. Chem.* **2000**, *65*, 4475−4481.

(21) Cohanoschi, I.; García, M.; Toro, C.; Belfield, K. D.; Hernández, F. E. Three-photon absorption of a new series of halogenated fluorene derivatives. *Chem. Phys. Lett*. **2006**, *403*, 133−138.

(22) Cronstrand, P.; Luo, Y.; Norman, P.; Agren, H. Ab initio calculations of three-photon absorption. *Chem. Phys. Lett.* **2003**, *375*, 233−239.